JOURNAL OF APPLIED POLYMER SCIENCE VOL. 9, PP. 2101–2119 (1965)

Some Relationships between Molecular Structure and Flow in Linear Polyethylene

H. P. SCHREIBER, *Central Research Laboratory, Canadian Industries Limited, McMasterville, Quebec, Canada*

Synopsis

The flow curves of linear polyethylenes are characterized by a set of empirically defined parameters, including the apparent melt viscosity at zero shear stress, the shear stress for onset of non-Newtonian flow, and the slopes of linear sections fitted to data in three shear stress ranges of the flow curve. Not all of these parameters have theoretical significance but all are easily measured and therefore should be useful for broad, practical application. The dependence of the parameters on molecular weight, shape, and breadth of the molecular weight distribution has been demonstrated by using fractions and blends of fractions of linear polyethylenes. The zero shear viscosity and degree of non-Newtonian flow at low shear stress depend primarily on polymer molecular weight. The degree of non-Newtonian flow at higher shear stress can be related quantitatively to molecular weight distribution factors, while the stress for onset of non-Newtonian flow also correlates with molecular weight distribution. Formally, the derived correlations are specific to the apparatus used, but may in fact have much broader validity because of the minor importance in these polymer samples, of elastic effects such as capillary die entry effects.

INTRODUCTION

A previous examination[1,2] of the melt viscosity–molecular weight relationship for linear polyethylene showed that non-Newtonian flow conditions were observed at progressively lower shear rates and stresses as the molecular weight increased above the critical entanglement molecular weight, M_c. The shear stress τ_1, at which the first significant decrease from the limiting zero stress melt viscosity was observed for a given sample, was suggested[2] for potential use as an indication of the average molecular weight in the high end of the distribution of a polymer sample. To test this concept further, blends of sharply fractionated linear polyethylenes were studied, with results reported in this communication.

A further purpose of this paper is to examine the dependence on molecular weight and molecular weight distribution of some empirical parameters which describe the flow curve of linear polyethylenes over appreciable shear stress ranges. The interdependence of flow behavior and molecular structure in polyethylenes is now a widely accepted principle,[3–7] several interesting attempts having been made to relate experimental results with theoretical concepts of non-Newtonian flow.[8,9] In re-examining the

relationship, emphasis is placed on empirically defined flow parameters which are readily measured even with relatively simple apparatus. Theoretical formality is thereby sacrificed to some extent for broadness and practicability of application.

EXPERIMENTAL

Materials

Phillips type linear polyethylenes were used as starting materials for fractionation by the large-scale coacervation method of Blackmore and Alexander.[10] Eleven fractions were used in this work. Their molecular structure data are given in Table I. Weight-average molecular weights

TABLE I
Characterization Data for Linear Polyethylene Fractions

Sample	$[\eta]$ (tetralin, 120°C.), dl./g.	$\bar{M}_w$ From $[\eta]$ and eq. (1)	$\bar{M}_w$ From light scattering	$\bar{M}_n$	$\bar{M}_w/\bar{M}_n = \Delta$
RF-1	0.170	3,500	—	~4,000	~1.0
RF-2	0.680	24,300	—	12,800	1.9
RF-3	0.939	38,100	—	24,500	1.6
RF-4	0.721	26,300	—	18,000	1.5
RF-5	1.22	55,000	—	29,000	1.9
RF-6	1.481	72,700	73,000	45,000	1.6
RF-7	1.923	105,000	100,000	—	—
RF-8	2.33	136,000	135,000	—	—
RF-9	2.41	158,000	155,000	74,000	2.1
RF-10	3.80	270,000	275,000	—	—
RF-11	~8.1	~800,000	—	—	—

$\bar{M}_w$ were obtained from light scattering in 1-chloronaphthalene solutions at 140°C., and from intrinsic viscosity measurements in tetralin solutions at 120°C., by using eq. (1),

$$[\eta] = 5.24 \times 10^{-4} \bar{M}_w^{0.71} \quad (1)$$

$\bar{M}_n$ values were obtained wherever possible from infrared measurements of vinyl unsaturation, assuming a 1:1 ratio of vinyl groups and polymer chain ends. For the higher molecular weight fractions, however, this method proved too insensitive to be useful. These latter samples were prepared by repeated refractionation steps, however, and it seems reasonable to assume therefore that the $\bar{M}_w/\bar{M}_n$ values, Δ, (final column Table I) are comparable to those of the lower molecular weight fractions.

Blended Fractions

Some of the simple fractions listed in Table I were blended to provide wide variations in the distribution factor Δ at constant $\bar{M}_w$ levels near

TABLE II
Composition and Characterization of Blended Linear Polyethylene Fractions

Sample	Composition	$\bar{M}_w$ Calculated	$\bar{M}_w$ From $[\eta]$ and eq. (1)	$\bar{M}_n$ (calculated)	Δ factor	Shape of distribution[a]
G_1B_1	28.7% RF-6, 71.3% RF-4	39,700	41,400	32,200	1.3	B
G_1B_2	95.6% RF-1, 4.4% RF-11	38,100	38,400	3,700	10.3	D
G_1B_3	31.9% RF-1, 9.6% RF-6 56.7% RF-4, 1.9% RF-11	38,200	35,700	8,800	4.1	A
G_1B_4	98.7% RF-4, 1.3% RF-11	36,400	38,300	26,700	1.4	C
G_2B_1	91.6% RF-1, 8.4% RF-11	70,000	70,000	3,800	18.4	D
G_2B_2	45.6% RF-9, 54.4% RF-1	73,000	71,800	6,300	11.6	C
G_2B_3	34% RF-9, 66% RF-3	78,200	78,000	51,300	1.5	B
G_2B_4	33% G_2B_2, 33% G_2B_3, 34% RF-6	80,300	80,300	20,200	4.0	A
G_3B_1	82.4% RF-1, 17.6% RF-11	144,000	141,000	4,250	33.2	D
G_3B_2	78.2% RF-3, 21.8% RF-11	203,000	145,000	48,000	3.0	C
G_3B_3	26.5% RF-6, 14.6% RF-3 17.5% RF-1, 27.7% RF-9 13.8% RF-11,	156,500	140,000	16,800	8.3	A
G_3B_4	33% RF-9, 51.4% RF-1 15.6% RF-11	168,000	151,000	6,700	22.5	D
G_4B_1	79.4% RF-1, 20.6% RF-11	170,000	240,000	4,400	54.5	D
G_4B_2	85.8% RF-6, 14.2% RF-11	176,000	213,000	83,300	2.6	B
G_4B_3	40% RF-6, 17.6% RF-9 27.5% RF-1, 14.9% RF-11	178,000	177,000	11,800	15.0	A

[a] A = broad, regular distributions; B = narrow distribution blend of fractions with similar $\bar{M}_w$; C = intermediate distribution blend of fractions with distinct $\bar{M}_w$; D = broad distribution blend of fractions with widely different $\bar{M}_w$.

4.0, 7.0, 15.0, and 22.0 $\times$ 10^4. Blended fractions are coded according to molecular weight group, as G_1, G_2, G_3, and G_4, respectively. Details of their composition are given in Table II. Blending was done by dissolving calculated amounts of sharp fractions in tetralin at 120°C., passing the solutions through a coarse sintered-glass plug, precipitating by methanol addition, then washing and vacuum drying the precipitate. Calculations of blend composition were based on the assumption that $\bar{M}_w$ of the blend was given by

$$\bar{M}_w = \sum w_i(\bar{M}_w)_i \tag{2}$$

where w_i is the weight fraction of the ith constituent. Experimental checks of the $\bar{M}_w$ value were made by intrinsic viscosity determinations. As shown in Table II, calculated and experimental $\bar{M}_w$ values generally are in good agreement, significant differences existing only in the higher molecular weight groups G_3 and G_4, where appreciable amounts of fraction 11 are used. Repeated viscosity measurements showed the $\bar{M}_w$ of this sample to be less accurately defined than in other cases.

Estimates of $\bar{M}_n$ for all but one of the blends were made from the relationship

$$M_n = [\sum w_i/(\bar{M}_n)_i]^{-1} \tag{3}$$

These values are not to be taken as absolute, since it was assumed for simplicity that each of the starting fractions was monodisperse. The $\bar{M}_n$ values in Table II therefore are used only to estimate relative broadening of the molecular weight distribution parameter Δ. The compromise procedure seems justified in the present context by the experimental difficulty of accurately determining $\bar{M}_n$ at high degrees of polymerization in polyolefins and by the relative invariance of Δ in the parent fractions.

Flow Parameters

Flow data were obtained at 190°C., by using the C—I—L high shear viscometer fitted, as in earlier work,[1,2] with flat entry dies having varying orifice diameters but constant length-to-radius (L/R) ratios of 7.64. No attempt was made to study capillary entry effects[11] in these cases. This omission does not seriously limit the general usefulness of results in these cases because, as has already been reported,[12] the magnitude of elastic effects (e.g., extrudate swelling) in these fractionated linear polyethylenes is very minor. Further, no significant capillary entry corrections were observed in earlier work with these and like materials.[12]

Logarithmic plots of the frequently defined[5,6] apparent melt viscosity η^* versus apparent shear stress at the capillary wall τ were constructed from the data, as shown by the typical example of Figure 1. The simple empirical parameters used in this work to characterize the flow behavior of polyethylene are also defined in Figure 1.

Low Shear Stresses. In the region approaching Newtonian flow conditions, the flow curve is characterized by the apparent Newtonian melt

viscosity η_0^*, the non-Newtonian flow rate β, and the shear stress for onset of non-Newtonian flow, τ_1. The former parameters are obtained from plots of melt fluidity ($1/\eta^*$) versus applied pressure, as shown in the insert of Figure 1. The stress τ_1 is determined by the arbitrary procedure[2]

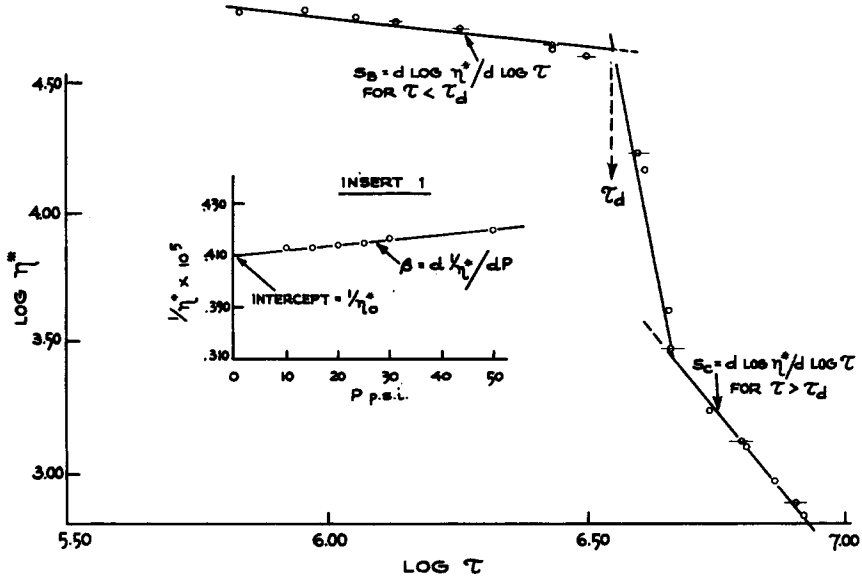

Fig. 1. Flow curve for RF-7 at 190°C. Definition of rheological parameters.

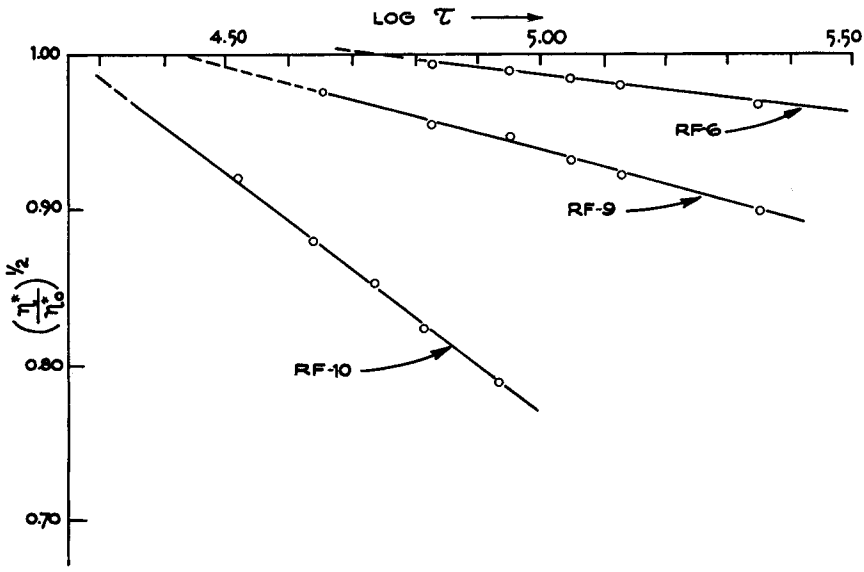

Fig. 2. Typical plots used to determine τ_1.

illustrated in Figure 2 by three typical examples, for values of the reduced viscosity parameter $(\eta^*/\eta_0^*)^{1/2}$ greater than about 0.8.

Higher Shear Stresses. Consistent with the aims of this work, empirical parameters were used to represent the flow curve on either side of the characteristic viscosity discontinuity[13-15] which conveniently divides the flow curve into two sections. In spite of some curvature in the flow curves it was found possible to fit straight lines over appreciable shear stress ranges on either side of the viscosity discontinuity. The slope, S_B, defined in Figure 1, is a measure of non-Newtonian flow in the shear stress range bounded by the critical stress τ_d at the "upper limit" of the discontinuity, and a stress roughly one decade lower. The experimental expedient was to include as many points as possible in the linear segment and calculate S_B by least-squares fit. The degree of non-Newtonian flow at stresses greater than τ_d was represented by the slope S_c of the straight line fitted to the points in this section of the flow curve (Fig. 1).

Measurements of post-extrusion swelling, indicative of melt elasticity in these materials, have been reported previously.[12] Plots of the swelling index B (defined as extrudate to die diameter ratio) versus log applied pressure were used to provide a compliance value B_p, and the swelling index at 200 psi, B_{200}, fixes the swelling plot in its coordinates.

RESULTS AND DISCUSSION

Effects of Varying Molecular Weight

The response of the empirical flow parameters to changes in $\bar{M}_w$ at roughly constant molecular weight distribution is shown by the data in Table III.

Newtonian Viscosity. Experimental values of η_0^* are compared with values calculated from the equation

$$\log (\eta_0^*)_{190} = 4.10 \log \bar{M}_w - 15.14 \tag{4}$$

defined earlier.[1] The agreement throughout is satisfactory, even in the case of sample RF10, where comparatively few data at very low shear stress necessitated a somewhat greater extrapolation to zero shear stress than was usually the case. Equation (4) is therefore applicable to the present fractions, which are less polydisperse than those used in the work defining the eq. (1).

Onset of Non-Newtonian Flow. A reciprocal variation between the shear stress for onset of non-Newtonian flow and $\bar{M}_w$ has been rationalized[2] and is again evident from the data in Table III. A correlation of $\bar{M}_w$ and the shear rate for onset of non-Newtonian flow in polyethylene has also been reported by Sabia.[16] The τ_1-$\bar{M}_w$ function is shown explicitly in Figure 3, where the choice of coordinates follows the precedent of earlier work[2] and the critical weight for chain entanglement, M_c, is equated to 4000.[1,9] For comparison the results for some of the fractions used in the

TABLE III
Rheological Parameters for Eight Polyethylene Fractions of Comparable Polydispersity

Sample	Newtonian η_0*, poise		Onset of non-Newtonian flow τ_1, dyne/cm.^{2}	Shear thinning parameters			Critical stress τ_d, dyne/cm.^{2}	Swelling parameters	
	Exptl.	Calc. [eq. (4)]		$\beta \times 10^8$	$-S_B$	$-S_C$		B_{200}[a]	B_p
RF-2	6.2×10^2	6.61×10^2	1.90×10^5	192	0.110	—	—	—	—
RF-3	$4.2_9 \times 10^3$	4.36×10^3	7.93×10^4	87	0.144	—	4.82	1.35	0.16
RF-5	$1.9_8 \times 10^4$	1.95×10^4	5.31×10^4	9.2	0.185	2.20	4.28	—	—
RF-6	6.15×10^4	6.17×10^4	5.10×10^4	8.0	0.204	2.72	4.36	1.31	0.15
RF-7	2.44×10^5	2.51×10^5	4.03×10^4	2.1	0.288	2.51	3.91	1.28	0.13
RF-8	$7.8_0 \times 10^5$	7.76×10^5	3.18×10^4	3.5	0.293	2.88	2.97	—	—
RF-9	1.28×10^6	1.38×10^6	2.71×10^4	1.6_5	0.315	2.43	4.24	1.17	0.03
RF-10	1.3×10^7[b]	1.31×10^7	1.70×10^4[b]	0.4_5	0.50	2.60	3.80	1.15	0.04

[a] Swelling index at 200 psi and 190°C.
[b] Estimates only, since data did not extend to sufficiently low stress for accurate extrapolation.

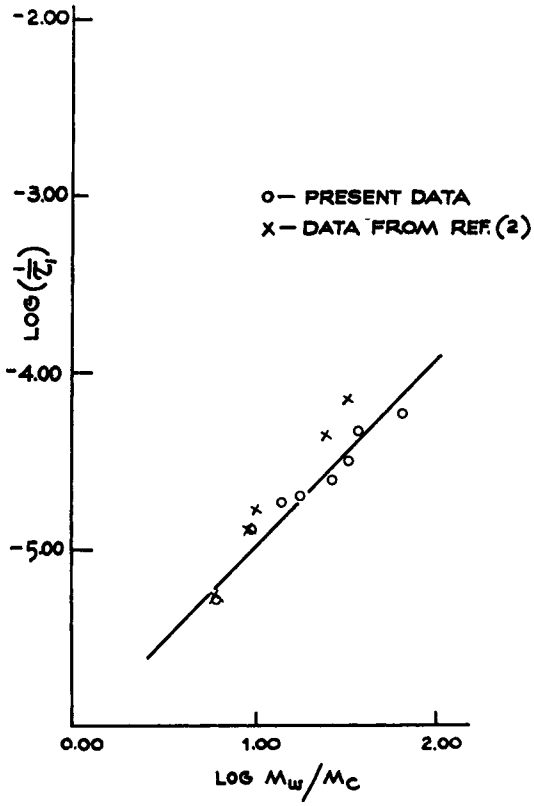

Fig. 3. Dependence of τ_1 on molecular weight for parent fractions ($\Delta \backsimeq 2$).

earlier work[2] are included in Figure 3. Because of reduced polydispersity the present results define a somewhat shallower line. This is expressed by the equation

$$1/\tau_1 = 10^{-6}(\bar{M}_w/M_c)^{1.03} \tag{5}$$

which will be used subsequently to calculate the molecular weight of the high molecular weight component in polydisperse linear polyethylenes from flow data at 190°C. The calculation may underestimate this molecular weight, since the present function refers to a sequence of polymers with $\Delta \simeq 2$. The limiting function for monodisperse systems would, presumably, shift toward more negative ordinate values at higher $\bar{M}_w/M_c$. Because the plot in Figure 3 must deviate from linearity at the abscissa origin and at high values of $\bar{M}_w/M_c$, eq. (5) must be restricted to the approximate range $5 < \bar{M}_w/M_c < 300$; this, of course, covers a major portion of generally available linear polyethylenes.

Degree of Non-Newtonian Flow. An increase in the degree of non-Newtonian flow with increasing molecular weight and increasing polydispersity has frequently been reported.[3-7] This may be a consequence of non-Newtonian flow conditions shifting to lower shear stresses, as suggested

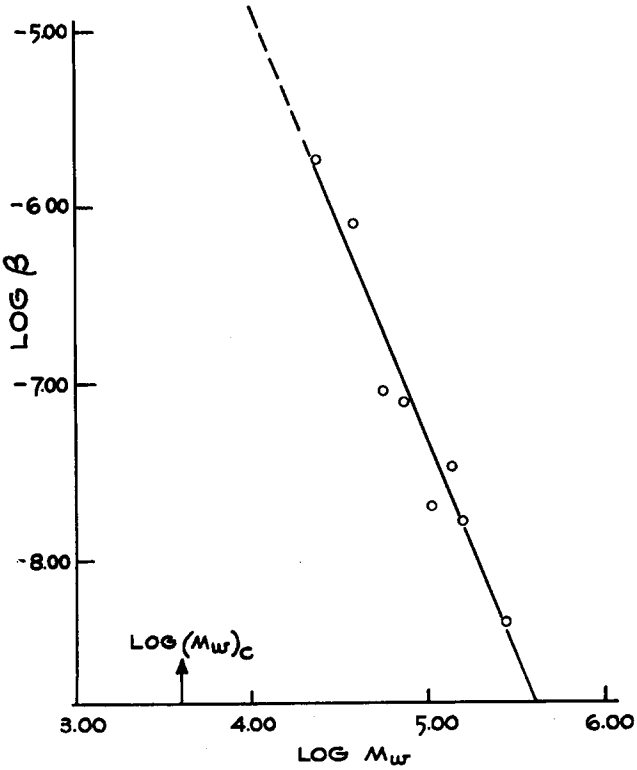

Fig. 4. Molecular weight dependence of flow parameter β.

by Porter and Johnson.[9] Present results further establish these interrelationships.

The simple empirical expression,

$$1/\eta^* = (1/\eta_0^*) + \beta P \tag{6}$$

where P is the applied pressure, adequately represents the viscosity–stress plot in the region near Newtonian flow conditions (see Fig. 1). The equation applies specifically to flow through a capillary orifice of defined dimensions and β is a convenient index of non-Newtonian flow in a restricted stress range. In view of the power dependence[17] between η_0^* and $\bar{M}_w$, an analogous dependence of β and $\bar{M}_w$ seems logical, and this is shown in Figure 4. The linear function is represented by

$$\beta = 1.26 \times 10^{-5}(\bar{M}_w/10^4)^{-2.47} \tag{7}$$

and eq. (7) is restricted to molecular weights greater than 10^4, since deviation from linearity must be expected as $\bar{M}_w \rightarrow M_c$, the critical weight for chain entanglement. Substituting eqs. (4) and (7) into eq. (6) gives

$$1/\eta^* = (7.24 \times 10^{-16}\bar{M}_w^{4.10})^{-1} + P[1.26 \times 10^{-5}(\bar{M}_w/10^4)^{-2.47}] \tag{8}$$

specific to flow through given dies, 190°C. and $\bar{M}_w > 10^4$.

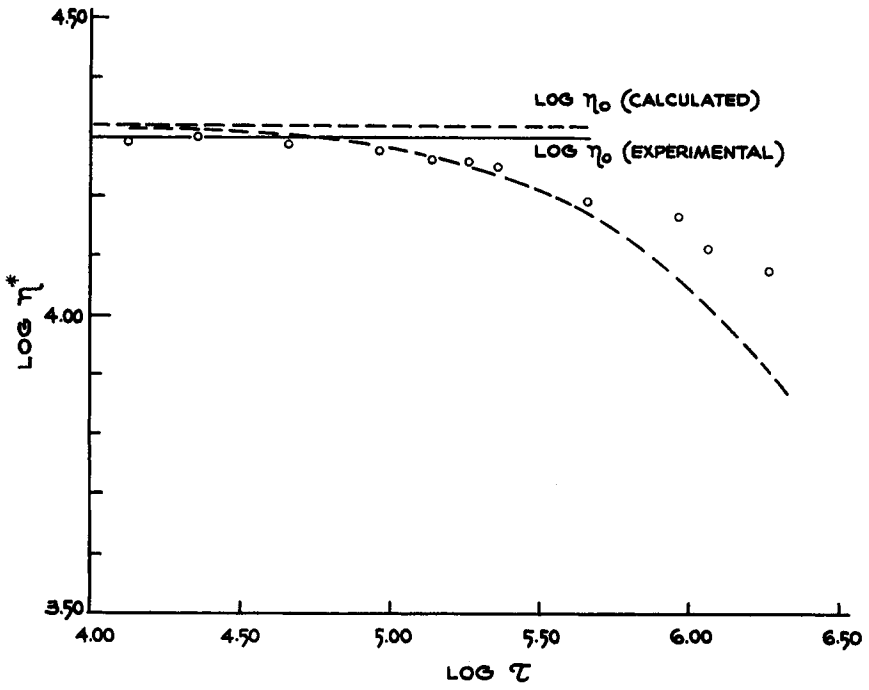

Fig. 5. Flow curve of fraction RF 5 at low shear stresses: (--) calculated from eq. (8); (O) experimental points.

The range of applicability of eq. (8) was checked by comparing experimental and calculated flow curves. A typical example is given in Figure 5 for fraction RF-5. Good agreement between calculation and experiment persists for about one decade of shear stress above the onset of non-Newtonian flow (τ_1). The range of applicability is, of course, in itself an indication of polydispersity in a given linear polyethylene sample.

While eq. (8) is formally valid only for dies with $L/R = 7.6$, practically it should closely approximate flow curves for other die geometries because of the virtual absence of elastic and die entry effects in these fractions.[12,19] The temperature variation of the relationship may be expected to follow the well known Williams-Landel-Ferry equation,[18] in analogy with findings of Wagner and Wissbrun.[4]

At shear stresses substantially greater than τ_1 the flow curve becomes more strongly dependent on the degree of polydispersity, as already indicated in Figure 5. Nevertheless, in a sequence of polyethylene samples where the degree of polydispersity is roughly constant, as in the eight samples here under examination, an evident dependence of the slope S_B on $\bar{M}_w$ is observed, as indicated in Figure 6. The relationship in Figure 6 is presumably one of a family, each specific to some constant breadth and shape of the molecular weight distribution, and therefore has no general applicability.

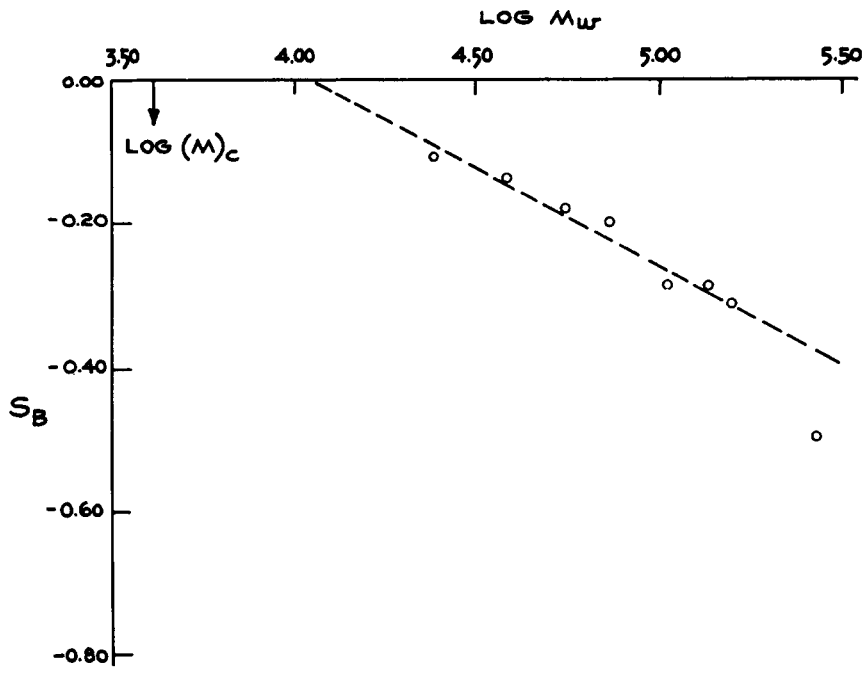

Fig. 6. Molecular weight dependence of slope S_B for parent fractions ($\Delta \simeq 2$).

There is little theoretical guidance to the structural dependence of the flow curve at stresses greater than τ_d. The data in Table III indicate that in these cases at least, the parameter S_c appears to be roughly constant.

Melt Fracture Stress and Extrudate Swelling. The values of the critical turbulence stress τ_d given in Table III vary somewhat but do not show the systematic inverse variation with molecular weight of whole polymers first noted by Spencer and Dillon[20] and subsequently by others.[21,22] The present results therefore correspond more closely with those of Mills et al.,[3] who also reported a critical stress essentially independent of polymer molecular weight.

In view of the significance of τ_d in terms of melt elasticity,[23] the present finding is regarded as another example of the drastic effects on melt elasticity brought about by the preparation history of the samples used. The previously noted[20–22] dependence of τ_d on molecular weight may be characteristic of the entangled polymer chain, τ_d representing the maximum deformation strain which can be withstood by the entanglement network without fracture. When chain entanglements are restricted or destroyed, for example by intensive solution history, the critical stress may be reduced to a material constant. The change in flow mode at τ_d in these cases may indeed be due to causes other than melt fracture, such as breakdown of adhesion of the polymer to the capillary wall resulting in a slip-stick flow mode.[14,24] This suggestion is an extension of arguments previously presented[12,19] to account for abnormally low extrudate swelling observed

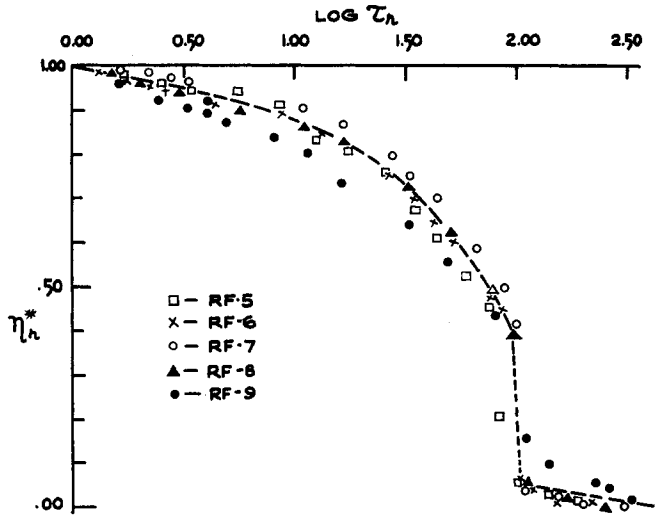

Fig. 7. Flow curve of polyethylene fractions of empirical reduced variables.

in these polyethylene fractions (viz., Table III) and the virtual absence in them of capillary entry effects. It also substantiates the identity of τ_d as a critical point in terms of the long range molecular interactions governing elastic behavior of the polymer melt, rather than in terms of shorter-range segmental interactions which seem to govern melt viscosity.[12,19]

Flow Curve on Reduced Variables. The preceding sections suggest that provided suitable compensation is made for differences in molecular weight and molecular weight distribution, the distinct flow curves of a family of polymer samples such as those involved here should reduce to a unique flow curve. The definition of reduced variables on the basis of flow theory is of course well known, Porter and Johnson's recent work[9] serving as an excellent example of the utility of such an approach. For consistency, however, reduced variables were defined in this case on the basis of the empirical parameters already introduced. Thus, molecular weight compensation is effected by the reduced viscosity $\eta_r^* = \eta^*/\eta_0^*$, and a reduced shear stress $\tau_r = \tau/\tau_1$ compensates for both molecular weight and molecular weight distribution, if a strong correlation between the shape and breadth of the molecular weight distribution function is assumed.

The reduced variables for five of the fractions listed in Table III were calculated by use of the η_0^* and τ_1 values entered there, and the resulting flow curves plotted in Figure 7. A narrow envelope of flow behavior is defined, with only the data for RF-9 deviating significantly from the mean. While the general usefulness of the present simple, empirical, definition of reduced variables cannot be assessed at this stage, it is obviously fully analogous in these cases to more cumbersome, theoretically based procedures and therefore holds promise for useful extension to other polymer systems.

Effect of Molecular Weight Distribution

The effects of varying molecular weight distribution on the flow properties of linear polyethylenes are indicated in Table IV (see Table II for details of the composition of the blended fractions used). Emphasis is given to the viscosity parameters, since extrudate irregularities made it difficult to obtain consistently reliable swelling data. The flow data are also not complete, since the present methods of measurement made it inconvenient to obtain low stress viscosities in series G_3 and G_4, and unreliable data appear to have been obtained at low shear for sample G_1B_2.

TABLE IV
Rheological Parameters for Blended Compositions Based on Polyethylene Fractions

	Newtonian flow region		Shear thinning region		
Sample	η_0^*, poise	τ_1, dyne/cm.^{2}	$\beta \times 10^8$	$-S_B$	$-S_C$
G_1B_1	3.1×10^3	4.4×10^4	140	0.207	0.92
G_1B_2	—	—	437	1.69	0.93
G_1B_3	4.8×10^3	5.2×10^3	260	0.42	1.15
G_1B_4	4.6×10^3	4.0×10^3	169	0.25	0.95
G_2B_1	$\sim 5.7 \times 10^4$	$\sim 6 \times 10^3$	199	2.24	1.80
G_2B_2	3.7×10^4	2.9×10^4	52.0	1.34	3.10
G_2B_3	4.1×10^4	3.1×10^4	17.5	0.24	2.90
G_2B_4	4.05×10^4	2.5×10^4	10.1	0.46	3.03
G_3B_1	—	—	150	2.24	—
G_3B_2	—	—	18	1.34	1.50
G_3B_3	—	—	5.8	1.15	1.62
G_3B_4	—	—	6.5	1.27	1.92
G_4B_1	—	—	15.5	3.66	3.4
G_4B_2	—	—	0.51	1.29	1.62
G_4B_3	—	—	0.56	1.29	1.61

In general, the data in Table IV confirm other published evidence that the degree of non-Newtonian flow in polyethylene and other thermoplastics increases with increasing molecular weight and broadening of the molecular weight distribution.[3-7] In terms of the logarithmic plot of melt viscosity versus shear stress the effect of molecular weight distribution is quite dramatic. This may be seen in Figure 8, which compares the flow curves of two G_3 blends with the target fraction of the group, RF-9. Evidently both the breadth and shape of the distribution function have a pronounced influence on the flow behavior of the polymers. It may be expected as a consequence that the interdependence of molecular weight, molecular weight distribution and flow parameters is complex and its quantitative formulation difficult.

Low Shear Stresses. Values of η_0^* and τ_1 could be measured with adequate accuracy for blends in groups G_1 and G_2 (see Table IV). The η_0^* values were used with eq. (4) to calculate $\bar{M}_w$ for the blends, and the calculated values compared in Table V with those obtained from intrinsic

TABLE V
Calculated and Actual Molecular Weight Parameters in Group 1 and 2 Blends

Sample	$\bar{M}_w \times 10^{-4}$		$(M)_{max} \times 10^{-4}$	
	Calculated from η_0* and Eq. (4)	Measured from $[\eta]$	Calculated from τ_1 and eq. (5)	Expected
G_1B_1	3.50	4.14	8.28	7.27
G_1B_3	3.90	3.57	66	~80
G_1B_4	3.86	3.83	85	~80
G_2B_1	~7.1	7.00	57	~80
G_2B_2	6.15	7.18	12.4	15.5
G_2B_3	6.38	7.80	11.7	15.5
G_2B_4	6.25	8.03	14.3	15.5

viscosities. The τ_1 data were used in conjunction with eq. (5) to compute $(M)_{max}$, the molecular weight of the high molecular weight constituent in each blend. These results are also entered in Table V and compared with $(M)_{max}$ values expected on the basis of the blend composition.

The agreement between $\bar{M}_w$ calculated from the apparent Newtonian viscosities and measured values is satisfactory considering the various possible sources of error in the experimentally complex comparison. The present results therefore confirm earlier suggestions[21] of relative independence between η_0* and molecular weight distribution. The agreement in Table V between expected $(M)_{max}$ data and those computed from τ_1 and eq. (5) is, on the whole, quite acceptable and confirms the usefulness of this shear stress parameter as an index of the high molecular weight tail in the distribution function of a polydisperse polymer.[2] In many practical cases a strong correlation can be expected between the high molecular weight segment of the distribution function and the overall breadth of the molecular weight distribution (e.g., the Δ factor), so that τ_1 should in those cases also correlate strongly with the breadth of the molecular weight distribution.

High Shear Stress Region. The increase in shear sensitivity of melt viscosity with increasing breadth of the molecular weight distribution is qualitatively evident from an inspection of the data in Table IV and II. The trend is similar to that reported by Döring and Leugering.[5] Figure 8 also shows the importance of the distribution shape factor. For example in G_3B_2 the change to a type C (apparently "bimodal") distribution with only a slightly higher Δ value than RF-9 itself results in a nearly fourfold increase in the slope S_B (viz., Tables II, III, and IV). The increase in non-Newtonian flow due to a broadening of the distribution to a type D in G_3B_1 is, of course, also obvious. A comparison of S_B and β values for G_4B_2 and G_4B_3 in Table IV further suggests the greater effectiveness of distributions based on fractions with widely different $\bar{M}_w$ constituents (type D blends, Table II) in increasing the shear sensitivity of the polymer melts.

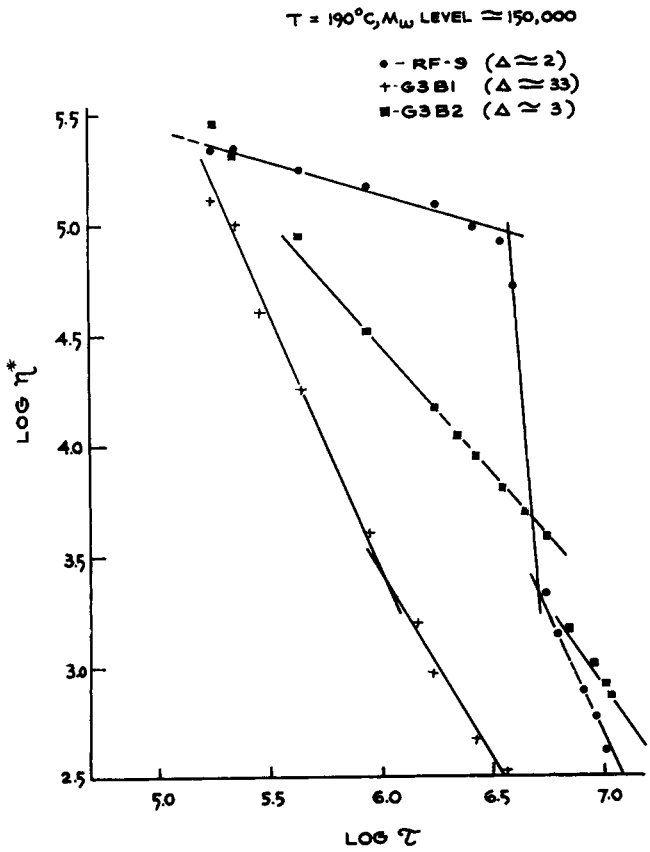

Fig. 8. Flow curves for polyethylenes with varying shapes and breadths of molecular weight distribution.

Although the influence of molecular weight distribution on degree of non-Newtonian flow is qualitatively evident, attempts to express the dependence quantitatively were only partly successful. No simple correlation between the low stress parameter β and molecular weight distribution could be derived, the β value retaining instead a strong link to $\bar{M}_w$ for the blends. A plot of β versus $\bar{M}_w/M_c$ in Figure 9 illustrates this. The influence of rising distribution width is of course evident in the deviation of data from the suggested relation, but except for fractions with broad, irregular distributions (type C or D), it is a reasonable approximation to regard β as a function primarily of $\bar{M}_w$, an appropriate statement of the function being eq. (7).

A logarithmic plot of absolute values of the slope S_B versus the distribution factor Δ, shown in Figure 10, indicates that the higher stress flow parameter correlates more strongly with the distribution factor. With the exception of the points for G_3B_2 and G_4B_2, the data fall on a readily defined line. The solid line in Figure 10 is not the true relationship be-

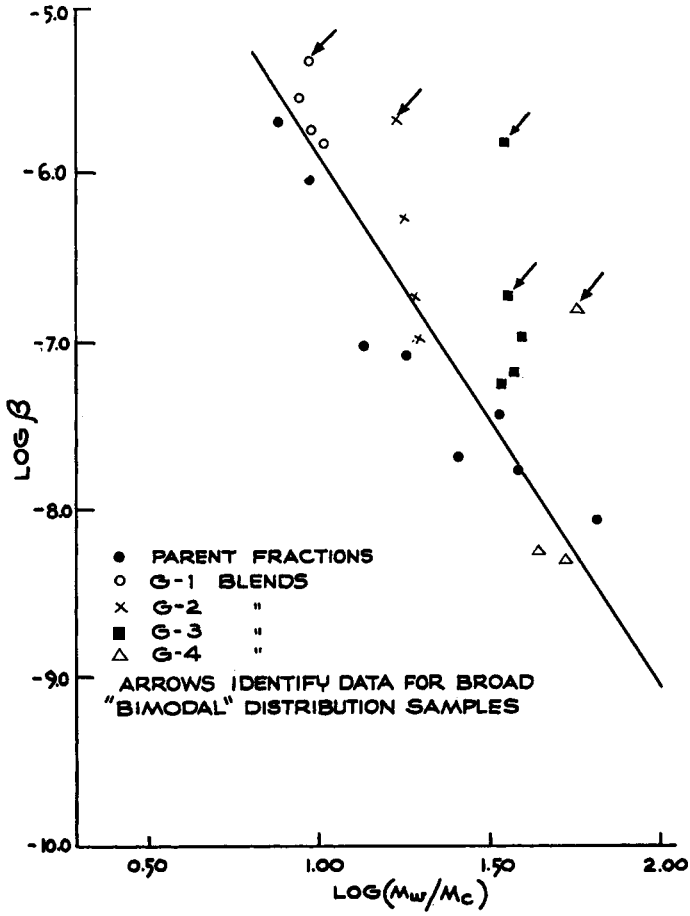

Fig. 9. Molecular weight dependence of flow parameter β for samples with various distribution shapes and breadths.

tween the variables, however, since the calculated Δ values assume monodispersity of the parent fractions. These had, in fact, Δ factors of the order of 2 (viz., Table I). A roughly constant shift factor should therefore be applied to the abscissa in Figure 10, and this is done (broken line) with the aid of data for five of the parent fractions. The equation relating to this line is

$$\log |S_B| = -1.0 + 0.78 \log \Delta \tag{9}$$

The correlation expressed by eq. (9) is far better than any between S_B and $\bar{M}_w$ alone. This is evident from the results in Table IV, where for any constant value of $\bar{M}_w$, S_B can vary over virtually the entire range of observed values. Thus, eq. (9) appears to relate an empirical flow parameter with a distribution function valid for varying shapes and breadths of the distribution over wide ranges of absolute molecular weight. It may also,

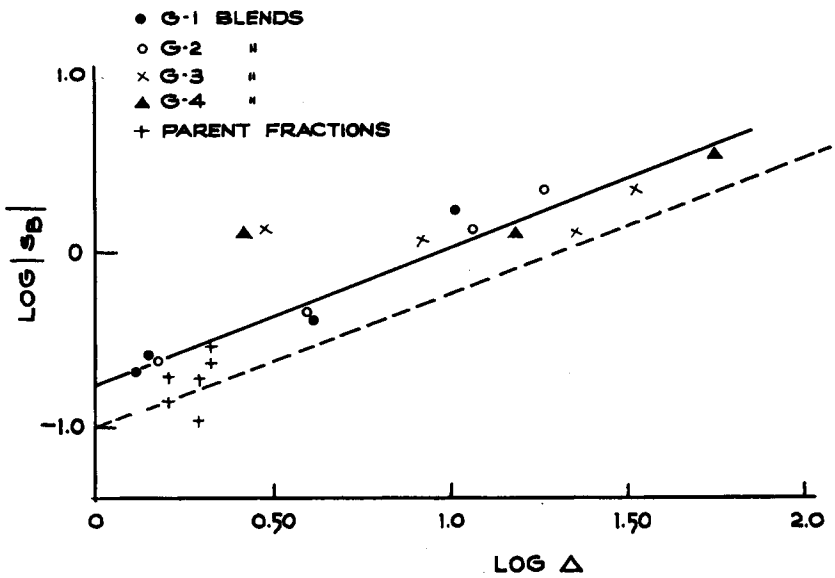

Fig. 10. Molecular weight distribution dependence of flow parameter S_B.

fortuitously, closely approximate an "absolute" relationship because of the earlier noted[12,19] absence of elastic and capillary entry effects in these polyethylenes, which would render their melt viscosities much less dependent on die length variations.[11]

The S_c slope data are entered in Table IV for completeness, but seem to follow no systematic trend. The random variations may be due to poor definition of experimental results; the experiments at these high shear stresses were indeed particularly troublesome because of the low melt viscosities attained.

CONCLUSION

Empirically defined, readily measured flow parameters have been used to gain a comprehensive picture of the molecular constitution of linear polyethylenes. The apparent zero shear melt viscosity and initial non-Newtonian flow rate β correlate with $\bar{M}_w$ via eqs. (4) and (7), respectively. The shear stress τ_1 for onset of non-Newtonian flow correlates with $\bar{M}_w$ of the high end of the distribution [eq. (5)] and therefore serves as a distribution shape factor. The slope S_B strongly correlates with the distribution factor Δ [eq. (9)] and therefore may also be useful in calculating $\bar{M}_n$ of the polymer. The critical stress τ_d is not clearly related to molecular size in these cases, however, and may signify changes in flow mode other than melt fracture. The stated correlations are formally valid only for the particular extrusion apparatus used in this study. In view of the reduced importance of elastic and capillary die entry effects in these polymers, however, their range of applicability may be more general.

References

1. Schreiber, H. P., E. B. Bagley, and D. C. West, *Polymer*, **4**, 355 (1963).
2. Schreiber, H. P., *Polymer*, **4**, 365 (1963).
3. Mills, D. R., G. E. Moore, and D. W. Pugh, *S.P.E. Trans.*, **1**, 40 (1961).
4. Wagner, H. L., and K. Wissbrun, *S.P.E. Trans.*, **2**, 222 (1962).
5. Döring, G., and H. J. Leugering, *Kunststoffe*, **53**, 11 (1963).
6. Guilett, J. E., R. L. Combs, D. F. Slonaker, D. A. Weemes, and H. W. Coover, Jr., paper presented at the 145th National American Chemical Society Meeting, New York, N. Y., Sept. 8–13, 1963.
7. Ferguson, J., B. Wright, and R. N. Haward, *J. Appl. Chem.*, **14**, 53 (1964).
8. Moore, L. D., Jr., paper presented at the 145th National American Chemical Society, New York, N. Y., September 8–13, 1963.
9. Porter, R. S., and J. F. Johnson, paper presented at the 4th International Congress on Rheology, Brown University, August 1963.
10. Blackmore, W. R., and W. Alexander, *Can. J. Chem.*, **39**, 1888 (1961).
11. Bagley, E. B., *J. Appl. Phys.*, **28**, 624 (1957).
12. Schreiber, H. P., and E. B. Bagley, *J. Polymer Sci.*, **B1**, 365 (1963).
13. Bagley, E. B., I. M. Cabott, and D. C. West, *J. Appl. Phys.*, **29**, 109 (1958).
14. Tordella, J. P., *J. Appl. Polymer Sci.*, **7**, 215 (1963).
15. Metzger, A. P., C. W. Hamilton, and E. H. Merz, *S.P.E. Trans.*, **3**, 21 (1963).
16. Sabia, R., *J. Appl. Polymer Sci.*, **8**, 1053 (1964).
17. Fox, T. G, S. Gratch, and S. Loshaek, in *Rheology*, Vol. 1, F. R. Eirich, Ed., Academic Press, New York, 1956, Chap. 12.
18. Williams, M. L., R. F. Landel, and J. D. Ferry, *J. Am. Chem. Soc.*, **77**, 3701 (1955).
19. Schreiber, H. P., A. Rudin, and E. B. Bagley, *J. Appl. Polymer Sci.*, **9**, 887 (1965).
20. Spencer, R. S., and J. E. Dillon, *J. Colloid Sci.*, **4**, 321 (1949).
21. Schreiber, H. P., and E. B. Bagley, *J. Polymer Sci.*, **58**, 29 (1962).
22. Knox, J. R., *Trans. Soc. Rheol.*, **7**, 418 (1963).
23. Bagley, E. B., *Trans. Soc. Rheol.*, **5**, 355 (1961).
24. Benbow, J. J., R. V. Charley, and P. Lamb, *Nature*, **192**, 223 (1961).

Résumé

Les courbes d'écoulement des polyéthylènes linéaires sont caractérisées par une série de paramètres définis empiriquement et comprenant la viscosité apparent à l'état fondu pour une force de cisaillement nulle, la force de cisaillement au commencement de l'écoulement non-Newtonien et les pentes des sections linéaires relatives à trois domaines de force de cisaillement de la courbe d'écoulement. Tous ces paramètres n'ont pas une signification théorique mais tous sont faciles à mesurer et, par conséquent, sont utiles pour une application large et pratique. La dépendance des paramètres par rapport au poids moléculaire, à la forme et à la largeur de la distribution du poids moléculaire, a été démontrée en employant des fractions et des mélanges de fractions de polyéthylènes linéaires. La viscosité pour un cisaillement nul et le degré de l'écoulement non-Newtonien à de faibles forces de cisaillement, dépendent principalement du poids moléculaire du polymère. Le degré de l'écoulement non-Newtonien à des forces de cisaillement plus élevées peut être relié quantitativement aux facteurs de distribution du poids moléculaire, tandis que la force pour le commencement de l'écoulement non-Newtonien est également en corrélation avec la distribution du poids moléculaire. Formellement, les corrélations déduites sont spécifiques à l'appareil utilisé, mais peuvent en fait avoir une validité beaucoup plus large à cause de l'importance minime, dans ces échantillons de polymère, des effets élastiques tels que les effets d'introduction capillaire.

Zusammenfassung

Die Fliesskurven linearer Polyäthylene werden durch eine Anzahl empirisch definierter Parameter charakterisiert, zu welchen die scheinbare Schmelzviskosität beim Schub null, Schubspannung für das Auftreten nicht-Newton'schen Fliessens und die Neigung von linearen, den Daten angepassten Abschnitten in drei Schubspannungsbereiche der Fliesskurve gehören. Nicht alle dieser Parameter besitzen theoretische Bedeutung, alle können jedoch leicht gemessen werden und sollten daher für eine breite praktische Anwendung brauchbar sein. Die Abhängigkeit der Parameter vom Molekulargewicht, der Gestalt und der Breite der Molekulargewichtsverteilung wurde an Fraktionen und Mischungen von Fraktionen von linearem Polyäthylen nachgewiesen. Die Viskosität beim Schub null und der Grad des Nicht-Newton-Fliessens bei niedriger Schubspannung hängen primär vom Molekulargewicht des Polymeren ab. Der Grad des nicht-Newton-'schen Fliessens bei höherer Schubspannung kann quantitativ zu Faktoren der Molekulargewichtsverteilung in Beziehung gesetzt werden, während die Spannung für das Einsetzen nicht-Newton'schen Fliessens ebenfalls zur Molekulargewichtsverteilung in Korrelation steht. Formal sind die abgeleiteten Korrelationen für den verwendeten Apparat spezifisch; sie können aber tatsächlich wegen der geringeren Bedeutung elastischer Effekte, wie kapillarer Formeingangseffekte, bei diesen Polymerproben eine viel grössere Gültigkeit besitzen.

Received October 5, 1964
Revised December 8, 1964